

JOURNAL

OF THE AMERICAN CHEMICAL SOCIETY

© Copyright 1984 by the American Chemical Society

VOLUME 106, NUMBER 3

FEBRUARY 8, 1984

A Novel Electrode for Electrochemical ESR and Its Application to Modified Electrodes

W. John Albery,* Richard G. Compton,† and Christopher C. Jones

Contribution from the Department of Chemistry, Imperial College, London, SW7 2AY, England.
Received March 4, 1983

Abstract: A tube electrode consisting of an incomplete annulus can be placed in the cavity of an ESR spectrometer without detuning the cavity. The ESR signals from the radical cation of *N,N,N',N'*-tetramethylphenylenediamine, produced by oxidation on a semiannular electrode at the center of the cavity, are shown to obey the solution to the convective diffusion equation, describing the transport of the radicals away from the electrode. Radicals in the coats of modified electrodes may be studied with the electrode at the center of the cavity. Studies on electrodes coated with poly(nitrostyrene) and with poly(vinylanthraquinone) are reported.

The combination of electrochemical generation and ESR detection¹⁻⁴ has been useful in elucidating intermediates and products in electrochemical reactions. In our work⁵⁻⁸ we have employed a tube electrode through which the solution flows under laminar flow as shown in Figure 1. Radical intermediates or products generated on the electrode are transported by the controlled flow through the cavity. The convective diffusion equation describing the transport and the concentration profile of the radical has been solved and the solution experimentally verified for a number of different cases, including those in which the radical is decomposing by either first- or second-order kinetics. With the electrode outside the cavity, the first-order and second-order rate constants must be less than 10 s^{-1} and $10^4 \text{ dm}^3 \text{ mol}^{-1} \text{ s}^{-1}$, respectively, for there to be a measurable ESR signal.

Radicals with shorter lifetimes could be detected if the generating electrode could be placed in the ESR cavity itself without detuning the cavity. In this paper we describe two simple electrode geometries by which this can be achieved. Unlike the ingenious helical electrode of Allendoerfer and co-workers,^{9,10} we still retain controlled and laminar flow of the solution past the electrode. With the electrode in the cavity one can also investigate radical species on the electrode itself. We describe two such studies on modified electrodes, where the electrode surface is coated with poly(nitrostyrene) or poly(vinylanthraquinone).

Results and Discussion

Electrode Geometry and Cavity Sensitivity. In Figure 2 we show how the sensitivity of our standard rectangular TE_{102} cavity to radicals varies with distance through the cavity. These measurements are made by positioning a tiny crystal of α, α' -diphenyl- β -picrylhydrazyl (DPPH) at various distances inside the tube that carries the electrolyte solution. With the tube electrode outside the cavity we obtain the expected \sin^2 profile for the sensitivity (curve a). Moving the annular electrode into the cavity

leads to curve b. The cavity is much less sensitive, and the \sin^2 curve is grossly distorted. Furthermore, the sensitivity is negligible in the vicinity of the electrode, and this was found to be the case wherever the electrode was placed inside the cavity. We have found that the sensitivity of the cavity can be maintained if instead of using a complete annulus for the tube electrode, one uses a half annulus. Curve c in Figure 2 shows the sensitivity when a semiannular tube electrode is placed at the center of the cavity, as shown in Figure 1. We now obtain the correct \sin^2 function. Compared to curve a, where the electrode was outside the cavity, the sensitivity is reduced by approximately one-half. However this is adequate for ESR measurements, and the electrode is now centered at the maximum in the sensitivity curve. The optimum orientation of the electrode with respect to the cavity is also shown in Figure 1; however, rotation of the electrode in the cavity affected the sensitivity by less than 10%. We have also investigated an annular electrode where a slice subtending 10° (the missing sector) has been removed. Curve d in Figure 2 shows the sensitivity when this electrode is placed at the center of the cavity. The \sin^2 function is now distorted, but the sensitivity at the electrode is enhanced by a factor of 3 compared to curve a.

The difference between a complete annular electrode and the semiannular, or missing-sector, electrodes is that in the former case the H_1 component of the standing microwave field will induce

- (1) Geske, D. H.; Maki, A. H.; *J. Am. Chem. Soc.* **1960**, *82*, 2671.
- (2) Adams, R. N. *J. Electroanal. Chem.* **1964**, *8*, 151.
- (3) Goldberg, I. B.; Bard, A. J. *J. Phys. Chem.* **1971**, *75*, 3281.
- (4) Goldberg, I. B.; Boyd, D.; Hirasawa, R.; Bard, A. J. *J. Phys. Chem.* **1974**, *78*, 295.
- (5) Albery, W. J.; Coles, B. A.; Couper, A. M.; Garnett, K. M. *J. Chem. Soc., Chem. Commun.* **1974**, 198.
- (6) Albery, W. J.; Coles, B. A.; Couper, A. M. *J. Electroanal. Chem., Interfacial Electrochem.* **1975**, *65*, 901.
- (7) Albery, W. J.; Chadwick, A. T.; Coles, B. A.; Hampson, N. A. *J. Electroanal. Chem. Interfacial Electrochem.* **1977**, *75*, 229.
- (8) Albery, W. J.; Compton, R. G.; Chadwick, A. T.; Coles, B. A.; Lenkait, A. J. *J. Chem. Soc., Faraday Trans. I* **1980**, 1391.
- (9) Allendoerfer, R. D.; Marticheck, G. A.; Bruckenstein, S. *Anal. Chem.* **1973**, *47*, 890.
- (10) Allendoerfer, R. D.; Carroll, J. B. *J. Magn. Reson.* **1980**, *37*, 497.

* Department of Inorganic, Physical, and Industrial Chemistry, Donnan Laboratories, Liverpool, L69 3BX, England.

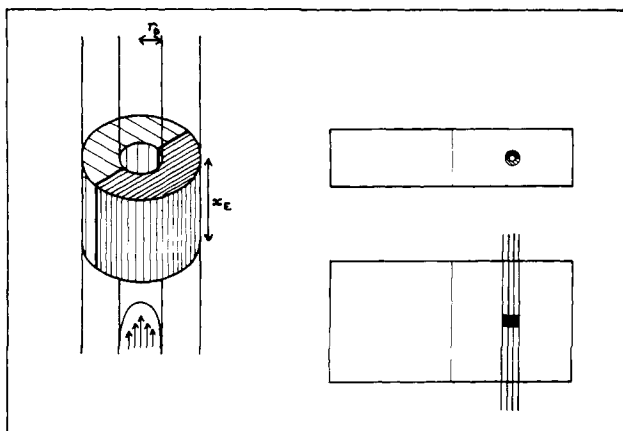


Figure 1. Semiannular tube electrode. The fine-hatched segment is made of platinum and the coarse-hatched segment of Teflon. The parabolic velocity profile is shown. In our case, the radius $r_0 = 0.50$ mm, and the length of the electrode, x_E , is 2.0 mm. The position of the electrode in the dual cavity is shown on the right-hand side of the diagram.

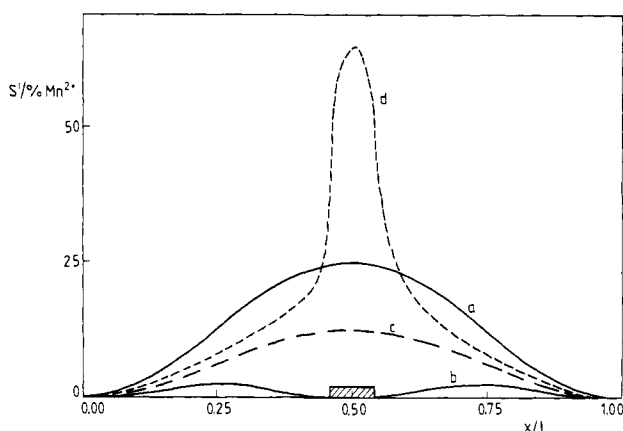
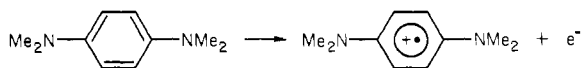


Figure 2. Variation of the sensitivity of the cavity with distance through the cavity. Curve a is obtained with no electrode inside the cavity; curve b is obtained with tube electrode consisting of a complete annulus at the center of the cavity as shown. Curves c and d are obtained with an electrode at the center of the cavity consisting of a half annulus and an annulus with a missing sector respectively.

eddy currents in the complete circle and therefore will not be able to penetrate to the electrolyte solution. By use of incomplete annuli the eddy currents are prevented. In the case of the semiannular electrode there is greater loss of sensitivity but the standing microwave field is preserved. For the missing-sector electrode the enhancement of sensitivity may be similar to that found by Lebedev,¹¹ who used a helical coil; the missing-sector electrode may be considered to be one turn of a helix. We consider that the semiannular electrode is better behaved than the missing sector electrode and have therefore used it for all of the work reported in this paper. However for applications where high sensitivity is required the missing sector electrode may be preferred.

Limiting Current. The behavior of the semiannular electrode was tested by using the oxidation of *N,N,N',N'*-tetramethyl-*p*-phenylenediamine (TMPD) in an aqueous solution containing 0.1 M K_2SO_4 :



Satisfactory voltammograms were obtained. The limiting current, i_L (for a semiannular electrode), is given by the Levich equation⁶

$$i_L = 2.75nFD^{2/3}x_E^{2/3}V^{1/3}c_\infty \quad (1)$$

where D is the diffusion coefficient, x_E is the length of the electrode, V is the volume flow rate, and c_∞ is the bulk concentration.

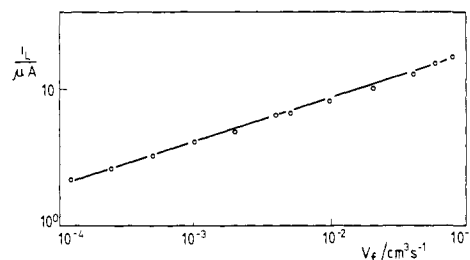


Figure 3. Variation of limiting current, i_L , with flow rate, V_f . In accordance with eq 1 the gradient of the log/log plot is $1/3$.

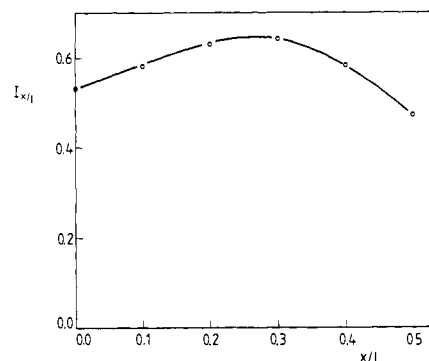


Figure 4. Variation of the numerical factor $I_{x/l}$ in eq 3 with distance through the cavity.

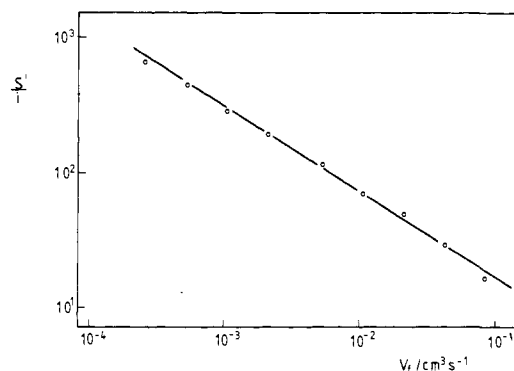


Figure 5. Variation with flow rate of the ESR signal for the semiannular electrode at the center of the cavity. In accordance with eq 2 the gradient of the log/log plot is $-2/3$.

Typical results for the limiting current as a function of flow rate are plotted according to eq 1 in Figure 3. A good straight line is obtained. From the intercept we find $D/\text{cm}^2 \text{s}^{-1} = 4.8 \times 10^{-6}$, which is in good agreement with results in the literature.¹² These results show that there are satisfactory hydrodynamic conditions at the electrode.

ESR Detection Efficiency. We have used the same system to test the ESR detection efficiency, $M_{x/l}$, where x is the distance of the electrode in the cavity and l is the length of the cavity. We assume that the length of the electrode (~ 2 mm) is much smaller than the length of the cavity (~ 2.4 cm). The concentration profile of the radical downstream of the electrode does not depend on the position of the cavity. Hence from our previous work⁶ the ESR signal, $S_{x/l}$, is given by

$$S_{x/l} = I_{x/l} S \cdot (l - x_E)^{2/3} r_0^2 i / nFD^{1/3} V^{2/3} \quad (2)$$

where r_0 is the radius of the tube, i the generating current, S , the ESR signal from a mole of spins at the center of the cavity, and $I_{x/l}$ a numerical factor that arises from convoluting the concentration profile with the sensitivity of the cavity. Figure 4 shows $I_{x/l}$ as a function of x/l , the position of the electrode in the cavity. In particular, for the electrode just outside the cavity, $I_0 = 0.53$,

(11) Lebedev, A. S.; Tararukha, O. M. *Teor. Eksp. Khim.* 1965, 1, 260.

(12) Philip, R. H. *J. Electroanal. Chem. Interfacial Electrochem.* 1970, 27, 369.

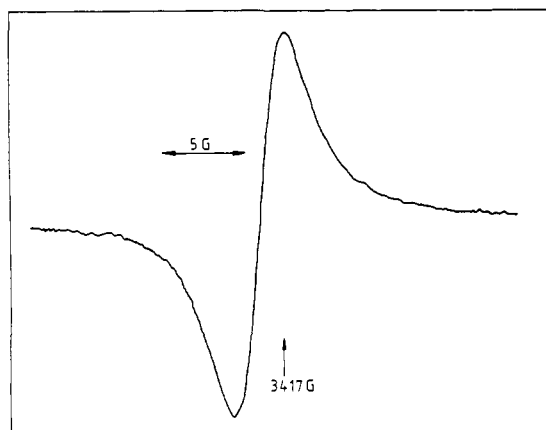


Figure 6. Typical ESR signal obtained on reducing the poly(nitrostyrene) electrode.

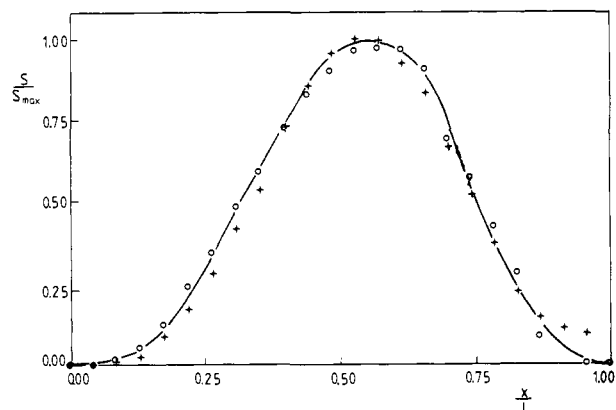


Figure 7. Variation with distance through the cavity of the ESR signal from a DPPH crystal (+) and from the modified electrode (O).

while when the electrode is at the center, $I_{1/2} = 0.47$.

When the semiannular electrode is used at the center of the cavity, results for $S_{1/2}$ as a function of flow rate are plotted according to eq 2 in Figure 5. The expected gradient of $-2/3$ is found.

In our previous work we defined the detection efficiency, $M_{x/l}$, so that it did not depend on either the size of the generating current or of the flow rate:

$$M_{x/l} = S_{x/l} V^{2/3} / i = I_{x/l} S \cdot (1 - x_E)^{2/3} r_0^2 / nFD^{1/3} \quad (3)$$

From the results in Figure 5 ($M_{1/2}$) and similar results with the electrode just outside the cavity (M_0), we find

$$M_{1/2} / M_0 = 0.48 \pm 0.03 \quad (4)$$

From the ratio of $I_{1/2}$ to I_0 given above and from the ratio of S_* , as measured by DPPH in Figure 2, we find

$$M_{1/2} / M_0 = 0.45 \quad (5)$$

Hence we can conclude that there is good agreement between theory and experiment for the ESR detection efficiency of the semiannular electrode placed at the center of the cavity. We estimate that with this configuration radicals with a lifetime as short as 1 ms should be measurable.

Poly(nitrostyrene)-Modified Electrode. We have also used the new type of electrode to examine radicals generated in the coats of modified electrodes. We used Miller's method¹³ to prepare a modified electrode consisting of platinum coated with poly(*p*-nitrostyrene), which we then examined in acetonitrile containing 0.2 M tetraethylammonium perchlorate (TEAP). Reduction at -1.60 V (with respect to Ag/0.01 M AgNO₃) produced the broad featureless ESR signal shown in Figure 6. The fact that this

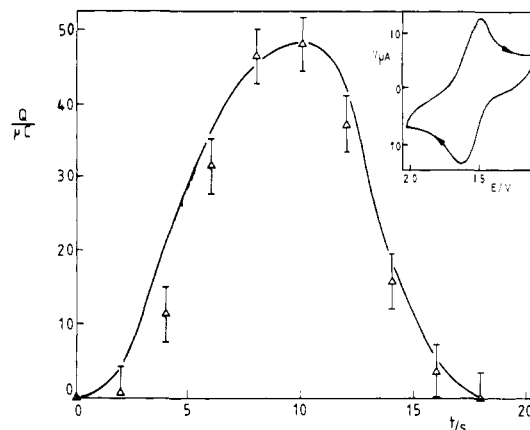


Figure 8. One cycle of a cyclic ESR intensity potential curve for the reduction and oxidation of poly(nitrostyrene). The points show the ESR signal while the curve is calculated by integrating the current of the cyclic voltammogram shown in the insert.

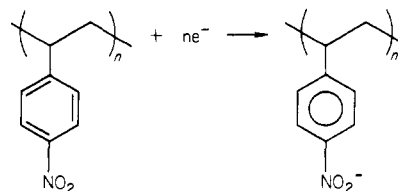
Table I. Variation of CV Peak Currents with Sweep Rate

sweep rate (P), mV s ⁻¹	i_a^a / P	i_c^b / P	$i_a^a / P^{1/2}$	$i_c^b / P^{1/2}$
20	0.25	0.30	1.1	1.3
50	0.19	0.23	1.3	1.6
100	0.14	0.17	1.4	1.7

^a Peak current (μ A) in anodic direction. ^b Peak current (μ A) in cathodic direction.

radical is bound to the electrode and is not in solution was shown by measuring the ESR signal strength as a function of the position of the electrode in the cavity. Results are shown in Figure 7. Excellent agreement is found with the results for the DPPH crystal taken from curve c of Figure 2.

By monitoring the maximum in Figure 6 one can measure the ESR signal intensity as one carries out a conventional cyclic voltammogram on the electrode. Typical results are shown in Figure 8. The ESR signal should match the charge injected into the coat:



For comparison purposes, in Figure 8 we therefore show the charge integrated from the cyclic voltammogram; reasonable agreement is found. When the sweep rate is varied, the peak height of the cyclic voltammogram is found to vary with the square root of the sweep rate. Results are given in Table I. This suggests that the amount of charge being injected is limited by transport processes in the coat. This conclusion is further confirmed by measuring the transient from a potential step from -1.4 V to -1.8 V. Approximately 10 times more charge can be injected by the end of the transient, showing that in the cyclic voltammetry only the inner layers are being reduced. When the potential is stepped from -1.8 V to -1.4 V the ESR signal decays as the anion is reoxidized. Results are shown in Figure 9. These results may be analyzed by using the same model as we have used for the thionine-coated electrode.¹⁴ We assume a rate-limiting diffusive process in a slab of finite width with no reaction taking place at the electrolyte interface. The expression for the current is

$$i = \left(\frac{D}{\pi t} \right)^{1/2} \frac{\Delta q}{l} \left\{ 1 + 2 \sum_{m=1}^{\infty} (-1)^m \exp \left(-\frac{m^2 l^2}{Dt} \right) \right\} \quad (6)$$

(13) Kerr, J. B.; Miller, L. L.; Van Der Mark, R. J. *Am. Chem. Soc.* **1980**, *102*, 3383.

(14) Albery, W. J.; Boutelle, M. G.; Colby, P. J.; Hillman, A. R. *J. Electroanal. Chem. Interfacial Electrochem.* **1982**, *133*, 135.

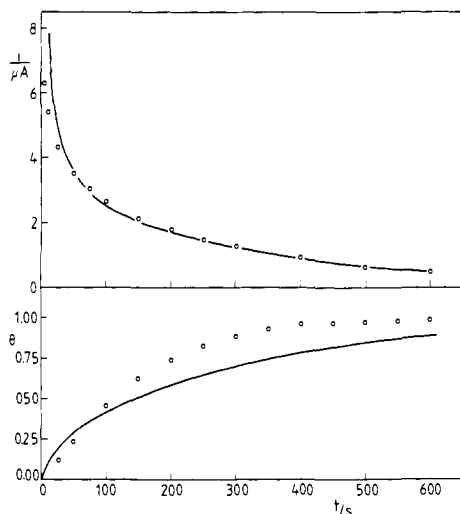


Figure 9. Current and ESR transients for the decay of the radical anion plotted according to eq 6 and 7, respectively.

where Δq is the total charge injected and l is the thickness of the coat. For the decay of the ESR signal we obtain

$$\theta = \frac{S_t - S_{t=0}}{S_{t=\infty} - S_{t=0}} = 2 \left(\frac{Dt}{l^2\pi} \right)^{1/2} + 2 \sum_{m=1}^{\infty} (-1)^m \times \left[2 \left(\frac{Dt}{l^2\pi} \right)^{1/2} \exp\left(-\frac{m^2 l^2}{Dt}\right) - 2m \operatorname{erfc}\left(\frac{ml}{D^{1/2}t^{1/2}}\right) \right] \quad (7)$$

As shown in Figure 9 reasonable agreement between theory and experiment can be found for

$$(D/l^2)/s^{-1} = 1.37 \times 10^{-3} \quad (8)$$

The fit for the ESR data (Figure 9b) is not as good as that for the current because the shape of the ESR spectrum changes with concentration; this effect will be discussed in a subsequent paper. The value of l may be found from the total charge/cm² of the layer, Δq , and the estimated volume, V' , of a single redox group, which we take to be 150 Å³.

$$l \approx \Delta q V' L / F = 4.0 \times 10^{-5} \text{ cm} \quad (9)$$

From eq 8 and 9 we obtain $D/\text{cm}^2 \text{ s}^{-1} = 2.2 \times 10^{-12}$. The value of D is typical of those found for transport in modified electrodes, but more work is needed to determine whether the rate-limiting process is electron transfer or counterion diffusion.

Poly(vinylanthraquinone)-Modified Electrode. In our search for possible electrodes to catalyze the reduction of dioxygen we have made poly(2-vinylanthraquinone). We have studied a platinum electrode coated with this polymer in dimethyl sulfoxide containing 0.20 M TEAP. The coat now contains a two-electron redox system:

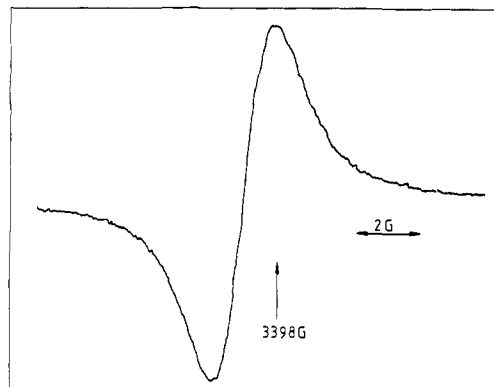
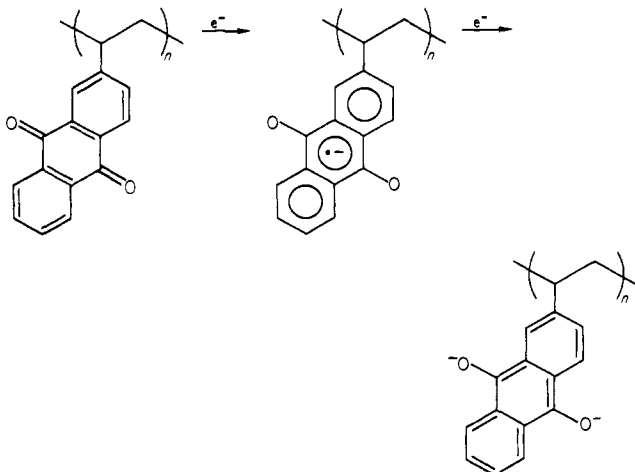


Figure 10. Typical ESR signal obtained on reducing poly(vinylanthraquinone).

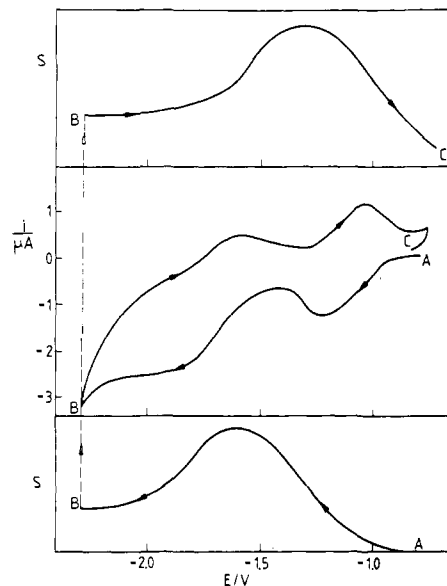


Figure 11. Cyclic esrogram for the poly(vinylanthraquinone) system. The middle section of the figure shows the cyclic voltammogram. The ESR signal resulting from semiquinone produced from reducing the quinone is shown in the curve AB at the bottom of the figure. At B the coat has largely been reduced to hydroquinone. The ESR signal resulting from semiquinone produced by oxidizing the hydroquinone is shown in curve BC at the top of the figure.

Figure 10 shows a similar broad featureless ESR signal seen when the coat is reduced at -1.40 V (with respect to $\text{Ag}/0.01 \text{ M AgNO}_3$). Typical cyclic voltammograms and cyclic esrograms are shown in Figure 11. It can be seen how the concentration of the semiquinone radical reaches a maximum between the two peaks of the cyclic voltammogram. This is to be expected since the radical is formed by the first electron transfer and destroyed by the second. Using both the charge and the ESR, as shown in Figure 11, one can then calculate the composition of the reduced species in the coat. Such detailed information will be most valuable in understanding the kinetics of charge transfer between redox groups in the coats of modified electrodes.

It is interesting that for both of the polymers studied so far we have obtained broad signals (Figures 6 and 10) with no fine structure. This may be because the radical centers cannot tumble fast enough in the polymer coat so that the ESR spectra are similar to those observed in a solid that contains so high a concentration of spins that the spectrum is dominated by strong exchange. For example, the spectrum of DPPH in the solid state has a width of 1.5–4.7 G,¹⁵ which is similar to those observed in our work. Another possibility is that the radicals are tumbling fast enough in the swollen polymer but that the hyperfine structure is destroyed

by electron exchange between the adjacent redox centers. Whichever explanation is correct, the new design of electrode should allow electrochemical ESR to be used first to study shorter lived intermediates and second to study intermediates and products in the kinetics of modified electrodes.

Experimental Section

The ESR spectrometer used was a Bruker ER 200 tt. The spectrometer has a dual cavity. In the second cavity a solid solution of Mn^{2+} in MgO serves as a permanent standard to calibrate the sensitivity of the spectrometer. The flow system and the method of construction of the tube electrode have been described previously.⁶ The nonelectroactive part of the semiannular or the missing sector electrodes was made of Teflon and assembled in the same way as a complete annular electrode. Except where stated, all chemicals and reagents were of AnalaR grade. Dimethylsulfoxide (BDH) was purified and dried as described previously.¹⁶ Acetonitrile (Fison's dried distilled) was refluxed with 1% (w/v) CaH_2 for 2 h and then fractionally distilled. TEAP (Fluka, purum) was recrystallized once from water. TBAT (Fluka, purum) was recrystallized once from a mixture of ethanol and petroleum ether. TMPD (BDH, L. R. grade) was recrystallized as described by Michaelis.¹⁷ Poly(nitro-

styrene) was synthesized by the method of Wiley and Smith.¹⁸ It was coated on to the platinum tube electrode by using the method of Miller.¹³

Vinylanthraquinone was synthesized by the method of Manecke and Storck.¹⁹ The monomer was polymerized by using benzoyl peroxide initiator in toluene solution at 100 °C for 240 h. The modified electrode was made by dip coating the platinum electrode in a 1% (w/v) solution of polymer in CH_2Cl_2 .

All electrochemical experiments were controlled by a purpose built potentiostat of modular construction.

Acknowledgment. We thank the SERC and the Wolfson Foundation for financial support. We are grateful to Mr. Michael Pritchard for his assistance in making the electrodes, to Mr. John Hooper for constructing the potentiostat, to Dr. S. Wilson for synthesizing poly(nitrostyrene), and to Mr. S. Jawaid for synthesizing poly(vinylanthraquinone). This is a contribution from the Wolfson Unit for Modified Electrodes.

Registry No. Pt, 7440-06-4; TMPD, 100-22-1; TMPD radical cation, 34527-55-4; poly(*p*-nitrostyrene), 24936-54-7; poly(*p*-nitrostyrene) radical anion, 87842-91-9; poly(2-vinylanthraquinone), 73546-39-1; poly(2-vinylanthraquinone) radical anion, 87842-93-1.

(16) Mann, C. K. *Electroanal. Chem.* **1969**, *4*, 57.

(17) Michaelis, L.; Schubert, M. P.; Granick, S. *J. Am. Chem. Soc.* **1939**, *61*, 1981.

(18) Wiley, R. H.; Smith, N. R. *J. Am. Chem. Soc.* **1950**, *72*, 5198.

(19) Manecke, G.; Storck, W. *Chem. Ber.* **1961**, *94*, 3239.

Electrocatalysis by Electrodeposited Spherical Pt Microparticles Dispersed in a Polymeric Film Electrode

Wen-Hong Kao and Theodore Kuwana*

Contribution from the Department of Chemistry, The Ohio State University, Columbus, Ohio 43210. Received May 9, 1983

Abstract: Electrochemical methods for the dispersion of Pt microparticles at microgram levels in polymeric matrices of poly(vinylacetic acid) glassy carbon electrodes, Pt-PVAA/GC, are described. The PVAA film was formed on a GC surface by refluxing neat VAA monomer under nitrogen. Cyclic voltammetry and single and double potential step electrolysis were applied to form the Pt^0 particles on PVAA/GC from an acidic hexachloroplatinate solution. The Pt particles were randomly dispersed in the polymer and were spherically shaped. This Pt-PVAA/GC electrode exhibited high activity toward the electrochemical generation of hydrogen and reduction of oxygen. Preliminary results indicate that the other catalytic electrodes based on a combination of substrates, polymers and electrochemically dispersed metals, mixed metals and metal/metal oxide particles can be generated by the same method.

Recently polymers have been used for the immobilization of redox mediators.^{1,2} They have also been used as supports for platinum catalysts which are in the form of thin films³ or dispersed colloids.⁴ Wrighton⁵ has used an ion exchange type polymer to disperse Pt^0 in the polymeric matrices via photoreduction or electrochemical reduction methods. This kind of modification

improves the efficiency of hydrogen evolution at p-type silicon semiconductor photocathodes.

Doblhofer and Durr⁶ have discussed two charge-transfer mechanisms for small particles dispersed in a polymer film on an electrode surface. One mechanism considers charge transfer to occur only at particles in contact with the electrode surface. The other is an electron-hopping mechanism.

Polymeric PVAA films have been formed on a GC surface at a monolayer coverage⁷ by a mechanical abrasion method⁸ or for thicker films by plasma polymerization.⁷ It has been discovered in this laboratory that a film can also be produced by refluxing the glassy carbon electrodes in the monomer.

The preparation and characteristics of a poly(vinylacetic acid) coated glassy carbon electrode with dispersed spherical platinum microparticles (Pt-PVAA/GC) are described. The application

(1) See discussions in the following: (a) Snell, K. D.; Keenan, A. G. *Chem. Soc. Rev.* **1979**, *8*, 259. (b) Murray, R. W. *Acc. Chem. Res.* **1980**, *13*, 135. (c) Albery, W. J.; Hillman, A. R. In "Annual Reports C"; The Royal Society of Chemistry: London, 1981. (d) Zak, J.; Kuwana, T. *J. Electroanal. Chem.* **1983**, *150*, 645.

(2) Gates, B. C. *NATO Adv. Study Inst. Ser. E* **1980**, *39*, 437.

(3) Katayama-Aramata, A.; Ohnishi, R. *J. Am. Chem. Soc.* **1983**, *105*, 658.

(4) Kiwi, J. "The Effect of Polymers on Dispersion Properties"; Tadros, Th. F., Ed.; Academic Press: London, 1982.

(5) (a) Bookbinder, D. C.; Bruce, J. A.; Dominey, R. N.; Lewis, N. S.; Wrighton, M. S. *Proc. Natl. Acad. Sci. U.S.A.* **1980**, *77*, 6280. (b) Dominey, R. N.; Lewis, N. S.; Bruce, J. A.; Bookbinder, D. C.; Wrighton, M. S. *J. Am. Chem. Soc.* **1982**, *104*, 467.

(6) Doblhofer, K.; Durr, W. *J. Electrochem. Soc.* **1980**, *127*, 1041.

(7) Tse, D. Ph.D. Thesis, The Ohio State University, 1980.

(8) Nowak, R.; Shultz, F. A.; Umana, M.; Abruna, H.; Murray, R. W. *J. Electroanal. Chem.* **1978**, *94*, 219.